VIII-II-1. Project Research

Project 4

PR4   Fundamental and Developmental Research on Physical and Chemical Characteristics of Actinides

H. Yamana

Research Reactor Institute, Kyoto University

1. Objectives and Allotted Research Subjects

Studies on actinide elements are categorized into two subjects, that is, a) engineering studies with the standpoint of nuclear fuel cycle, and b) fundamental studies with the standpoint of physics and chemistry. National laboratories are directed to the engineering vocation, while university laboratories are permissible to concentrate on the basic research. The principal objective of the present project research is to provide scientific and technological basis of physics and chemistry of actinide elements. Thus it covers various experimental studies of actinides and transactinides, on nuclear properties, radiochemical and other chemical properties, process chemistry, and material properties, and so on. Allotted research subjects are as the followings.

ARS-2 Study on coordination chemistry of actinide elements (Y. Ikeda *et al.*).

ARS-3 Isotope production and application by using actinides (S. Shibata *et al.*)

ARS-4 Spectroelectrochemical analysis of actinide ions in molten salts (A. Uehara *et al.*)

ARS-5 Study on chemical isotope effect of actinides and fission product elements (T. Fujii *et al.*).

ARS-7 Thermodynamic study of actinide complexes in aqueous solution (T. Sasaki *et al.*).

ARS-8 Fundamental study on solid-state properties of perovskite type oxides (S. Yamanaka *et al.*).

ARS-9 Assessment study on chemical properties of actinides in molten salts (M. Myochin *et al.*).

ARS-10 Electrochemical study of uranium in pyrochemical reprocessing system (M. Kurata *et al.*).

ARS-11 Basic study for "atom at a time chemistry" of heavy actinide and trans-actinide elements (A. Shinohara, *et al.*)

2. Main Results and Contents

Nuclear physical properties of TRUs were investigated in the study, ARS-3. The preparation of ^{243}Am target was performed by precipitation method as neutron-irradiation target for measurements of neutron-induced fission cross-sections. ARS-2, ARS-4, ARS-9, and ARS-10 studied the chemical behavior of actinides in molten salt and ionic liquid systems, the results of which are to be dedicated to the development of reprocessing technique. ARS-2 studied electrochemical properties of uranyl nitrate complexes in an ionic liquid. Cyclic volatmmograms of uranyl nitrate complexes in 1-R-3-methyl-imidazolium nitrates [R = ethyl (EMIN), R = butyl (BMIN)] were obtained. ARS-4 studied the redox reaction of the $NpO_2^+|NpO_2$ couple in molten NaCl-CsCl eutectic at 923 K. Cyclic voltammograms and absorption spectra of NpO_2^+ were measured to study coordination circumstance of neptunium ions in the melt. ARS-9 studied redox behavior of U in molten Li_2MoO_4–Na_2MoO_4 eutectic. The cyclic volatmmograms were precisely analyzed. ARS-10 studied electrolytic reduction of UO_2 in LiCl-Li_2O system. The reduction rate of UO_2 was found to be almost twice as high at 973 K as at 923 K. ARS-5 and ARS-7 studied the chemical behavior of actinides in aqueous solutions. ARS-5 studied the coordination circumstance of NpO_2^{2+} in concentrated nitrate solution by Raman spectrometry. The symmetric ν_1 vibration of O=Np=O was found. In ARS-7, as a reference of Th(IV), the hydrolysis of Zr was studied. The zirconium solubility in the presence of oxalic and malonic acid was measured in a wide range of hydrogen ion concentration (pH$_c$) and carboxylic acid (C2x) concentration. In ARS-8, electrical conductivity measurements on (Sr,Ba)MoO$_3$ and (Sr,Ba)MoO$_4$ were performed. The magnitude relations in the thermal conductivities among SrMoO$_3$, BaMoO$_3$, SrMoO$_4$, and BaMoO$_4$, based on the Wiedemann-Franz relation were discussed. In ARS-11, the extraction behavior of Ac(III), Am(III), Cm(III), and Cf(III), into di(2-ethylhexyl)phosphoric acid (HDEHP) was studied. The tetrad effect between the lanthanide and actinide series was discussed.

3. Summaries of the achievements

In this research, by using various unique facilities of KURRI for actinide research, new and characteristic chemical and nuclear physical data were obtained. These new information encompass solid chemistry, molten salt and solution chemistry, as well as nuclear reactions of actinides. The results are useful either for scientific purpose or for technological purpose for actinide management in the nuclear fuel cycle.

PR4-1   **Electrochemical Studies on Uranyl Nitrate Complexes in1-Alkyl-3-Methylimidazolium Nitrate Ionic Liquids**

S. Kim[1], N. Ohta[2], Y. Morita[1], N. Asanuma[3], K. Takao[4] and Y. Ikeda[1]

[1] *Japan Atomic Energy Agency, Tokai-mura, Naka-gun, Ibaraki 319-1195, Japan*
[2] *Research Laboratory for Nuclear Reactors, Tokyo Institute of Technology, 2-12-1-N1-34 O-okayama, Meguro-ku, Tokyo 152-8550 Japan*
[3] *Department of Energy Science and Engineering, School of Engineering, Tokai University 1117 Kitakaname, Hiratsuka-shi, Kanagawa 259-1292 Japan*
[4] *Institute of Radiochemistry Forschungszentrum Dresden-Rossendorf (FZD) P.O. Box 510119 D-01314 Dresden, Germany*

INTRODUCTION: Ionic liquids (ILs) have been paid attention as environmentally benign media, because ILs have attractive properties such as thermal stability, non-flammability, high ionic conductivity, and wide electrochemical potential windows [1,2]. In the nuclear industry field, ILs are expected to be used as reaction media in the reprocessing processes and the radioactive waste treatments, *i.e.*, media for pyro-reprocessing, liquid-liquid extraction, electrodeposition, and so on [1-4]. Present study was performed to obtain basic data on electrochemical properties of uranyl nitrate complexes in ILs.

EXPERIMENTS: Cyclic voltammograms of 1-R-3-methyl-imidazolium nitrates [R = ethyl (EMIN), R = butyl (BMIN)] containing of uranyl nitrate complexes were measured using an electrochemical analyzer (BAS, ALS model 660B) in a glove box under an Ar atmosphere at 50 ± 1 °C. A glassy carbon (BAS, diameter = 1 mm), a Pt wire, an Ag/AgCl electrode (BAS, RE-1B) with a liquid junction filled with ILs were used as a working, a counter, and a reference electrodes, respectively. All potentials reported here are *vs.* Ag/AgCl. The EMIN and BMIN were prepared by mixing EMI or BMI bromides with aqueous solution of $AgNO_3$ and purified by conventional method. The resulting EMIN and BMIN were kept for more than 3 h under reduced pressure at 120 °C to remove water. Sample solutions were prepared by dissolving uranyl nitrate into these ILs. Water in samples was removed as mentioned above.

RESULTS: The cyclic voltammograms of EMIN solution containing uranyl nitrate are shown in Fig. 1. As seen from this figure, two peaks corresponding to one redox couple were observed around –0.43 (E_{pc}) and –0.22 V (E_{pa}) in EMIN system. The potential differences between two peaks (ΔE_p) are 209 and 218 mV at 80 and 200 mV/s, respectively, and much larger than the theoretical value (62 mV) for the reversible one electron transfer reaction at 50 °C. Furthermore, the values of (E_{pc} + E_{pa})/2 is constant, –0.324 ± 0.002 V, regardless of *v*. These results suggest that uranyl(VI) species in EMIN is reduced to uranyl(V) quasi-reversibly and that the formal redox potential (E^o) is –0.324 V. On the other hand, in BMIN system, uncoupled cathodic peaks were observed around –0.64 V. This suggests that uranyl species in BMIN may be reduced to uranyl(V) irreversibly. The resulting uranyl(V) species seems more stable in EMIN than in BMIN.
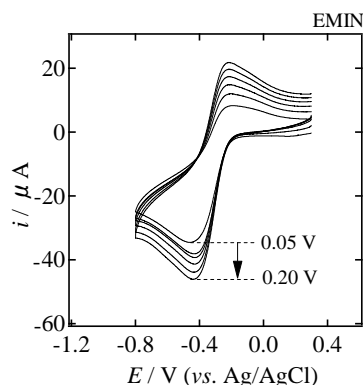

Fig. 1. Cyclic voltammograms of EMIN containing uranyl nitrate measured at various scan rates. Temp. = 50 °C, [U(VI)] = 0.125 mol/dm^3.

REFERENCES:
[1] P. Giridhar, K.A. Venkatesan, *et al.*, *Radiochim. Acta* **94** (2006) 415.
[2] V.A. Cocalia, K.E. Gutowski, R.D. Rogers, *Coord. Chem. Rev.* **250** (2006) 755.
[3] N. Asanuma, M. Harada, Y. Yasuike, M. Nogami, K. Suzuki, and Y. Ikeda, *J. Nucl. Sci. Technol.* **44** (2007) 368.
[4] Y. Ikeda, K. Hiroe, N. Asanuma, and A. Shirai, *J. Nucl. Sci. Technol.*, **46** (2009) 158.

Target Prepararion of ^{243}Am by Precipitation Method

K. Takamiya and H. Kikunaga[1]

Research Reactor Institute, Kyoto University
[1] Graduate School of Science, Osaka University

INTRODUCTION: Fission cross section is one of the most fundamental data in operating nuclear reactors and treating nuclear waste safely. For a safety evaluation of fast breeding reactor system, the cross section data of minor actinides (MA's) which are produced in nuclear reactors by neutron capture reaction of nuclear fuel elements is important parameters. But, measurements of the cross sections of neutron capture and fission reactions are difficult because of in-purities contained in MA samples those are produced in the samples by nuclear decay of the MA's. Therefore, in the measurement of nuclear properties of MA's, careful preparation of an MA sample is required. Furthermore, the sample preparation should be carried out just before the examination. The target preparation of ^{237}Np and ^{241,243}Am was tried in the previous report [1] and cross section measurements for these MA's have been performed using a electron linear accelerator in KURRI. But in the measurement for ^{243}Am, observed cross section values includes an effect of the in-purity of ^{239}Pu ($T_{1/2}$ = 24,110 y) which is daughter nucleus of ^{243}Am ($T_{1/2}$ = 7,370 y) because the long time interval between the target preparation and the cross section increased daughter nuclei in the target. In this work, the preparation of ^{243}Am target was tried again by precipitation method [2, 3] as neutron-irradiation target for measurements of neutron-induced fission cross-sections.

EXPERIMENTS: Chemical treatment for separating daughter nucleus of ^{239}Pu was performed before the preparation of ^{243}Am as an irradiation target. The procedure of chemical separation was basically the same as the previous preparation [1]. A part of the original solution containing 1.0 mg of ^{243}Am in about 700 μg acidic solutions was poured to the anion exchange column (Muromac 1X8). In order to elute americium only, an eluting solution (1 mL of 9 M HCl) was injected to the column. Most plutonium adsorbed in the column. The eluting solution was poured to the next anion exchange column, and americium was eluted by the same eluting solution again. The amount of ^{239}Pu was checked after each elution step by alpha-particle spectrometry. After three times of purification, americium was precipitated by adding NH$_4$OH and filtered by Anodisc. The precipitation filtered on the Anodisc was dried up, and alpha-particle spectroscopy was carried out to determine the amount of ^{243}Am and in-purities.

RESULTS: The alpha-particle energy spectra of the prepared ^{243}Am targets is shown in Fig. 1. Upper and lower panels show the spectra of the targets prepared in the present and previous works, respectively. The resolution of energy spectrum in this work is not better than that in the previous work because more purification steps could increase organic in-purity in the prepared target which increases energy loss of alpha-particles in the target. But, from the width of each energy peak, the prepared targets is thin enough to detect fission fragments emitted from the target using PPAC fission chamber for a cross section measurement. The ratio between ^{243}Am and ^{239}Pu was similar to the previous work. The amount of ^{243}Am prepared as the irradiation target in the present work is determined as 27 μg.

The cross section measurement for ^{243}Am has been performed soon after the preparation of the target, and there is less effect of in-purities in the observed data compared to the previous measurement.
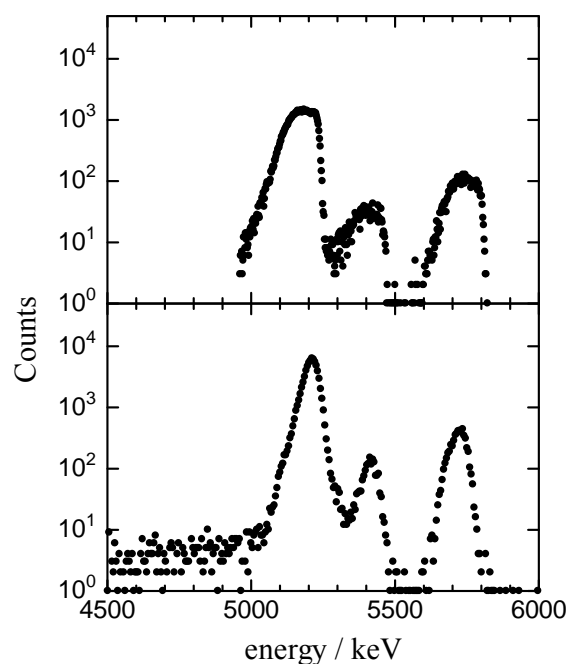

Fig. 1. The alpha-particle spectra of ^{243}Am targets. Upper and lower panel show the spectrum of the ^{243}Am targets prepared in the present and previous works, respectively.

REFERENCES:
[1] K. Takamiya, H. Kikunaga
KURRI Progress Report **2008**, 117.
[2] H. Kikunaga, Y. Kasamatsu, K. Takamiya, T. Ohtsuki, H. Yuki, A. Yokoyama, T. Nakanishi and T. Mitsugashira
Applied Radiation and Isotopes, **67** (2009) 539-543.
[3] K. Takamiya, T. Ohtsuki, H. Yuki, T. Mitsugashira, N. Sato, T. Suzuki, M. Fujita, T. Shinozuka, Y. Kasamatsu, H. Kikunaga, A. Shinohara, S. Shibata, T. Nakanishi: Applied Radiation and Isotopes **65** (2006), 32-35.

PR4-3　　Redox Reaction of the NpO_2^+|NpO_2 Couple in Molten NaCl-CsCl Eutectic

A. Uehara[1], T. Nagai[2], T. Fujii[1] and H. Yamana[1]

[1] *Research Reactor Institute, Kyoto University*
[2] *Nuclear Fuel Cycle Engineering Lab., Japan Atomic Energy Agency*

INTRODUCTION:

To recover from high level wastes, it is important to study chemical behavior of uranium and plutonium ions as well as minor actinides (MAs; neptunium Np, americium Am, curium Cm etc.). In our group, the redox potential and absorption spectra of uranium and plutonium ions in molten NaCl-CsCl eutectic have been reported [1]. For Np, which is one of the long-lived MAs, however, there are few reports for the redox reaction of the NpO_2^+|NpO_2 couple. In the present report, the redox reaction of the NpO_2^+|NpO_2 couple in molten NaCl-CsCl eutectic were studied based on the cyclic voltammograms, and absorption spectra of NpO_2^+ was measured to study coordination circumstance of neptunium ions in the melts at 923 K.

EXPERIMENTAL:

The valence of Np ion in molten salt was controlled by flowing Ar and/or Cl_2 gas through the sample cell Neptunium ion in the molten salt and monitored in-situ spectrophotometric measurement. A single beam spectrophotometer V-350 (JASCO Co. Ltd.) was used for the absorption spectrophotometry over the wave length range from 400 to 2000 nm. After the preparation of NpO_2^+ was determined by absorption spectra, electrochemical measurement was carried out. Two graphite rods of 3 mm in diameter were used as working and counter electrodes, and a reference electrode was an Ag|Ag$^+$ electrode composed a PYREX tube, about 1 g of 4.85 mol% AgCl in NaCl-CsCl eutectic, and an Ag wire. An electrochemical measurement system, HAG-5001 (Hokuto Denko Co. Ltd.) was used for the measurement of the formal redox potential of the NpO_2^+| NpO_2 couple.

All the experiments were carried out in a glove box filled with dry argon whose humidity and oxygen impurity was continuously kept less than 1 ppm.

RESULTS:

The NpO_2Cl was prepared from NpO_2 by passing through Cl_2 gas for 30 min at 20ml min^{-1} in NaCl-CsCl eutectic. NpO_2 was oxidized by Cl_2 as following reaction;
NpO_2 + 1/2 Cl_2 → NpO_2Cl
Absorption spectrum corresponding to NpO_2^+ was observed as shown in Fig. 1. Absorption bands observed in the NaCl-CsCl eutectic were similar to that in LiCl-KCl eutectic [2]. Assuming that stability of coordination structure is depended on the molar absorptivity, this result indicates that the coordination structure of NpO_2^+ in NaCl-CsCl eutectic is more stable than that in LiCl-KCl eutectic.
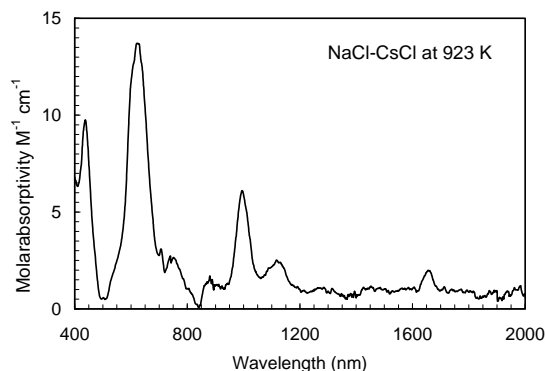

Fig. 1. Absorption spectrum of NpO_2^+ in NaCl-CsCl eutectic at 923K.

Cyclic voltammogram for the redox of the NpO_2^+|NpO_2 couple was observed in the temperature of 923 K as shown in Fig. 2. A cathodic peak current corresponding to the reduction of NpO_2^+ was proportional to the square root of the potential scanning rate between 0.01 and 0.1 V s^{-1}. It was found that the electrode reaction was controlled by the diffusion of NpO_2^+. However, the redox reaction of the NpO_2^+|NpO_2 couple was irreversible reaction because of the potential shift of cathodic peaks. Mid-point potential of the NpO_2^+|NpO_2 couple was calculated to be -0.41 ± 0.02 V vs. Ag|Ag$^+$ suggesting that the redox potential of the NpO_2^+|NpO_2 couple was close to that of the UO_2^+|UO_2 couple. Based on the results obtained, recover of Np and U is considered to be feasible as oxides in the reprocessing process.
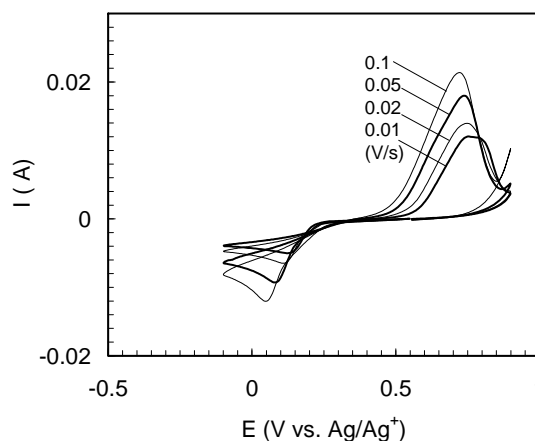

Fig. 2. Cyclic voltammogram for the redox of the NpO_2^+|NpO_2 couple in NaCl-CsCl eutectic at 923K.

REFERENCES:

[1] T. Nagai, *et al.*, Radiochim. Acta, **97**, (2009) 209.
　　J. Nucl. Sci. Techol., **42**, (2005) 1025.
[2] R.Lusy, *et al.*, Bull Soc. Chim. Belg., **83**, (1974) 227.

PR4-4 **Chemical Separation of TRU Elements and Fission Products and Their Isotopic Fractionations in the Separation Process**

T. Fujii, S. Fukutani and H. Yamana

Research Reactor Institute, Kyoto University

INTRODUCTION: Hydrate melts (fused hydrated salts) are known as extremely highly concentrated electrolytes. Because of the limited amount of water, the water activity is as small as that of concentrated HNO_3. Extraction of some *f*-elements by TBP from hydrate melts has been performed (see references in [1]). We have interests in the system with calcium nitrate hydrate melts, $Ca(NO_3)_2 \cdot RH_2O$, with water content R less than about 6. In the present study, we investigated the chemical behavior of neptunium (^{237}Np) in $Ca(NO_3)_2 \cdot RH_2O$ by Raman spectrometry.

EXPERIMENTAL: A HCl solution including ^{237}Np was once dried by heating on a hot plate, then the chloride was converted to nitrate by evaporation in concentrated nitric acid. $Ca(NO_3)_2 \cdot RH_2O$ ($R = 4.0$ or 8.0) containing ~0.01 M Np were prepared. 1 M HNO_3 solution containing the same amount of Np was also prepared. 0.4 mL of each solution was transferred into a quartz cell having a 2 mm light path, and this cell was sealed. The Raman scattering was collected at 90° to the incident beam. Raman spectra were obtained by an excitation using the 514.5 nm of an Ar^+ laser (NEC, GLS3280 and GLG 3280) and recorded by a JASCO NR-1100 spectrophotometer at 0.2 cm^{-1} intervals and 120 cm^{-1}/min scanning rate. The laser power at the sample was 400 mW.

RESULTS: Generally, disproportionation of Np(V) to Np(IV) and Np(VI) is considered in the Np/nitric acid system. Valence of Np in the hydrate melts was confirmed by UV/Vis/NIR absorption spectrometry. The electronic absorption spectra of Np(III), Np(IV), Np(V), and Np(VI) in HNO_3 solutions have been measured in a pioneering study [2]. According to the reported spectrum of Np(IV) in 1 M HNO_3, its characteristic absorption peak is positioned at ~700 nm with a molar absorptivity $\varepsilon \approx 70$ M^{-1} cm^{-1}. No peak at 700 nm is found in our results, and hence, the valence state of Np in hydrate melts should be higher than Np(IV). From the reported molar absorptivities [2], if the ratio of molar absorptivities (Np(V)/Np(VI)) is similar to the 1 M HNO_3 case, [Np(VI)] should be larger than [Np(V)] in hydrate melts.

Raman spectrometry is an effective analytical method to determine the coordination circumstance of cations and anions in $Ca(NO_3)_2 \cdot RH_2O$ [3]. Figure 1 shows Raman spectrum of 0.01 M Np in $Ca(NO_3)_2 \cdot 4.0H_2O$. The ν_1 symmetric vibration of NpO_2^{2+} can be seen in 850~870 cm^{-1} region, whose intensity is much smaller than that of the ν_4 vibration of NO_3^- in <760 cm^{-1} region (700~750 cm^{-1}). The lower frequency vibration around 720 cm^{-1} is known as the vibration of free NO_3^-, which is hydrated. The higher one, around 740 cm^{-1} is the vibration of bound NO_3^- coordinated to cations [3].
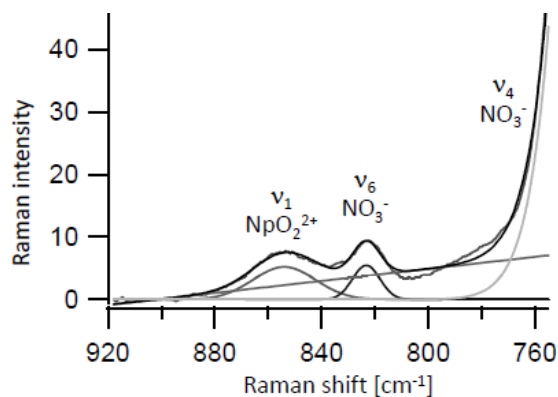

Fig. 1. Raman spectrum of Np in a calcium nitrate hydrate melt, $Ca(NO_3)_2 \cdot 4H_2O$.

The ν_1 symmetric vibrational frequency of NpO_2^{2+} in a $HClO_4$ solution has been reported to be 863 cm^{-1} [4]. A frequency of 859.4 cm^{-1} was found for our 1 M HNO_3 system, and this should be the ν_1 frequency of NpO_2^{2+}. Neptunyl ions in $Ca(NO_3)_2 \cdot 4H_2O$ (Fig. 1) showed a vibrational frequency at 854.0 cm^{-1}. This would be attributable to the ν_1 frequency of NpO_2^{2+}, nevertheless the frequency was smaller than that found in the 1 M HNO_3 system.

REFERENCES:
[1] T. Fujii *et al.*, IOP Conf. Ser. Mater.: Sci. Eng., **9** (2010) 012061(7 pages).
J. Nucl. Sci. Technol., **32** (1995) 1230-1235.
[2] H. A. Friedman and L. M. Toth, J. Inorg. Nucl. Chem., **42** (1980) 1347.
[3] T. Fujii *et al.*, J. Nucl. Sci. Technol., suppl. **3** (2002) 336.
[4] L. J. Basile *et al.*, Appl. Spectrosc., **28** (1974) 142.

PR4-5   Zirconium Solubility in Ternary Aqueous System of Zr(IV)-OH-Carboxylate

T. Sasaki, T. Kobayashi, S. Aoyama, H. Yoshida, H. Moriyama[1], T. Fujii[1] and H. Yamana[1]

Department of Nuclear Engineering, Kyoto University
*[1]Research Reactor Institute, Kyoto University*

INTRODUCTION: Zr(IV) solubility in the presence of oxalic and malonic acids has been discussed[1,2]. Among many kinds of organic acids, multidentate chelating ligand is one of the most important ligands, due to its strong coordination capability. Oxalic (C20) and malonic (C21) acids, which are considered as simple model ligands of various organic acids, can form stable and strong bidentate complexes with tetravalent ions. It is also known that precipitates form on adding oxalic and malonic acid to solutions of zirconium and thorium. In the present study, the zirconium solubility in the presence of oxalic and malonic acid was measured in a wide range of hydrogen ion concentration (pH_c) and carboxylic acid (C2x) concentration. Similar to the case in the absence of the carboxylic acid, size distributions of soluble species were obtained by sequential filtration.

EXPERIMENTAL: A stock solution of zirconium was prepared from perchlorate salt which was obtained from $ZrCl_4$ by perchloric acid fuming in a Teflon beaker covered with a watch glass. Aliquots of the stock solution were added to oxalic acid or malonic acid solutions such that the initial Zr concentration was 0.01 mol/dm^3 (M). The ionic strength (I) was set as 0.5 by the addition of $NaClO_4$, and the pH_c value was adjusted by adding $HClO_4$/NaOH. After aging the sample solutions at 25 °C, the pH_c values of the supernatants were measured. The supernatants were filtered through Microcon centrifugal filters.

RESULTS: Figs. 1 and 2 show the plots of zirconium solubility after filtration with 3k Da NMWL membranes in the presence of C20 and C21, respectively. The solubility of amorphous zirconium hydroxide ($Zr(OH)_4$(am)) in the absence of C2x is also shown for the purpose of comparison (broken line). The plotted values with downward facing arrows in Fig. 2 indicate the solubility data near the detection limit. No significant change was observed in the zirconium solubility even after a few months, indicating that steady state was achieved. Since there was no significant difference between the solubility after filtrated through 3, 30, and 100 kDa NMWL, it was assumed that the dominant species were "mononuclear" species. In the presence of C21 at pH_c 5.8, on the other hand, the solubility would increase with the increasing pore size of the filters. The formation of colloids by hydrolysis reaction might occur under this condition.

In the presence of 0.1 M C20 below pH_c 6.0, no precipitate was observed, indicating that the precipitate was dissolved due to the formation of anionic species. As shown in Fig. 1, the zirconium solubility in this case was observed to be higher than that in the absence of C20 under weakly acidic and near neutral conditions. In the

presence of 0.02 M C20, the solubility at about pH_c 7 was lower than that below pH_c 6. This can be explained by the strong hydrolysis reaction in the high pH region. However, in the presence of 0.1 M C20, no decrease of the solubility at the same pH_c was observed due to the strong complex formation of zirconium oxalate. Similarly to the C20 system under weakly acidic conditions, the solubility in the presence of C21 was found to be higher than that in the absence of C21 but was lower than that in the presence of C20. This suggests the possible formation of anionic malonate complexes. In the presence of 0.005 M C20 and C21, in which the concentration of the carboxylic acids was quite low, no increase of the zirconium solubility was observed compared to that in the absence of C2x. On the other hand, the zirconium solubility with C21 under acidic conditions was obviously lower than that of hydroxide, as shown by the broken curve in Fig. 2. The solubility of zirconium in the presence of C21 under acidic conditions might be controlled by a zirconium-malonate in the solid phase instead of $Zr(OH)_4$ (am).
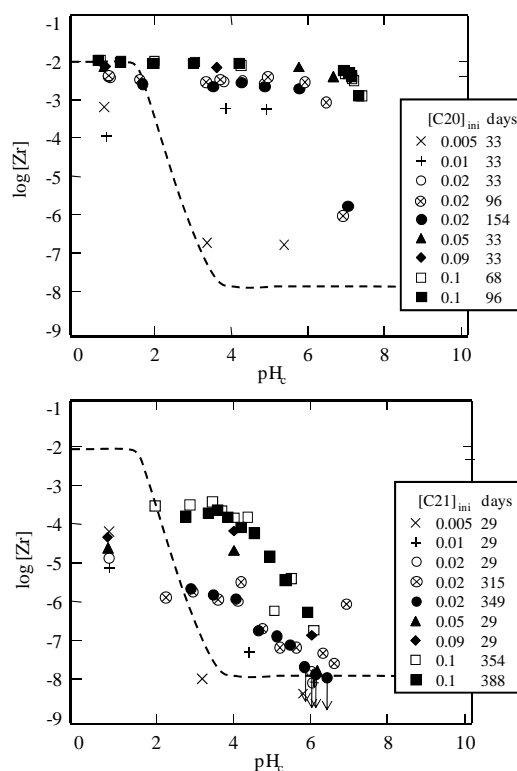
Figs. 1 and 2   Zirconium solubility after 3k Da filtration in the presence of C20 and C21 prepared by the oversaturation method. The dashed curve represents the solubility of zirconium hydroxide without C2x.

REFERENCES:
[1] Kobayashi, et al., Radiochim. Acta., **97** (2009) 237.
[2] Kobayashi, et al., J. Nucl. Sci. Technol., **46** (2009) 142.

PR4-6   Electrical Conductivity Measurment and Thermal Conductivity Analysis on (Sr,Ba)MoO$_3$ and (Sr,Ba)MoO$_4$

S. Yamanaka[1,2], M. Uno[2], K. Kurosaki[1] and H. Muta[1]

[1]*Division of Sustainable Energy and Environmental Engineering, Graduate School of Engineering, Osaka University*
[2]*Research Institute of Nuclear Engineering, University of Fukui*

INTRODUCTION: The behavior of fission products and the properties of their compounds are very important for evaluation of the fuel characteristics. The gray oxide phase of (Sr,Ba)-(U,Pu,Zr,RE,Mo)-O compounds have been observed as the oxide inclusions. In our previous study, we performed thermal conductivity characterizations on the (Sr,Ba)-Mo-O ternary compounds and revealed that the thermal conductivities of (Sr,Ba)MoO$_3$ are approximately 10 times higher than those of (Sr,Ba)MoO$_4$. In the present study, we performed electrical conductivity measurements on (Sr,Ba)MoO$_3$ and (Sr,Ba)MoO$_4$ to explain the magnitude relations in the thermal conductivities among SrMoO$_3$, BaMoO$_3$, SrMoO$_4$, and BaMoO$_4$, based on the Wiedemann-Franz relation.

EXPERIMENT: High-density sintered samples of SrMoO$_3$, BaMoO$_3$, SrMoO$_4$, and BaMoO$_4$ were prepared. The electrical conductivity of the samples was measured in the temperature range from room temperature to 950 K in a He atmosphere.

RESULTS: Figure 1 shows temperature dependence of the thermal conductivities (κ) of (Sr,Ba)MoO$_3$ and (Sr,Ba)MoO$_4$, in the temperature range from room temperature to 950 K. Clearly, κ values of (Sr,Ba)MoO$_3$ are quite high compared with those of (Sr,Ba)MoO$_4$. The values are 30 Wm^{-1}K^{-1} at room temperature, which is approximately 10 times higher than those of (Sr,Ba)MoO$_4$. One of the reasons of this high κ would be the electronic contributions. It is well known that the total thermal conductivity (κ_{total}) of solids is mainly composed of two components: lattice thermal conductivity (κ_{lat}) and electronic thermal conductivity (κ_{el}). We roughly calculated the κ_{el} of (Sr,Ba)MoO$_3$ and (Sr,Ba)MoO$_4$ based on the Wiedemann-Franz relation using the Lorenz number ($L = 2.45 \times 10^{-8}$ WΩK^{-2}), i.e. $\kappa_{el} = L\sigma T$, where σ is the electrical conductivity. The σ data of (Sr,Ba)MoO$_3$ are shown in Fig. 2. It was confirmed that the σ of both compounds are relatively high and de-

crease with temperature, like metals. At 300 K, the κ_{el} are calculated to be 4.9 Wm^{-1}K^{-1} and 10.5 Wm^{-1}K^{-1} for SrMoO$_3$ and BaMoO$_3$, respectively. On the other hand, the σ values of (Sr,Ba)MoO$_4$ are vanishingly small, so the κ_{el} could be treated as zero. At 300 K, the κ_{lat} (= κ_{total} - κ_{el}) are 25.8, 19.7, 3.5, 1.9 Wm^{-1}K^{-1} for SrMoO$_3$, BaMoO$_3$, SrMoO$_4$, and BaMoO$_4$, respectively. It can be said that the exceptionally high κ of (Sr,Ba)MoO$_3$ is caused by not only their high κ_{el} but also their intrinsically high κ_{lat}.
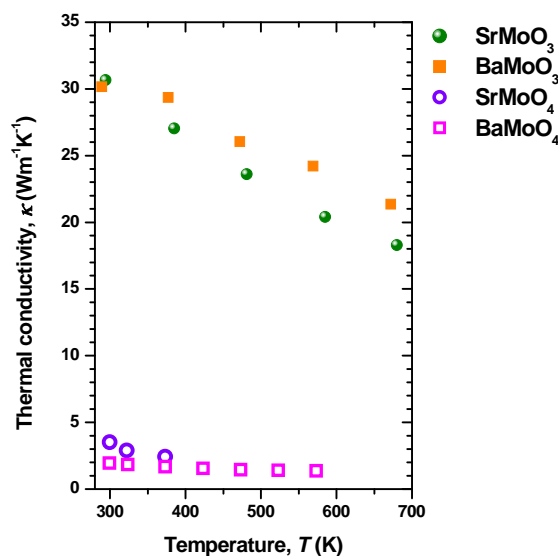

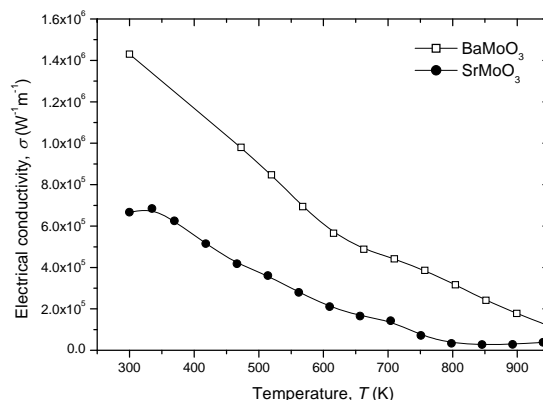Fig. 1. Temperature dependence of the thermal conductivities of (Sr,Ba)MoO$_3$ and (Sr,Ba)MoO$_4$.

Fig. 2. Temperature dependence of the electrical conductivities of (Sr,Ba)MoO$_3$.

PR4-7   **Study on Chemical Property of Actinide Ions in Molten Salts**

T. Nagai, M. Fukushima, A. Uehara[1], T. Fujii[1],
M. Myochin and H. Yamana[1]

Japan Atomic Energy Agency (JAEA)
[1]Research Reactor Institute, Kyoto University

INTRODUCTION: A pyrochemical process by using an alkaline molybdate melt has been studied as a promising reprocessing process for spent nuclear oxide fuels. This alkaline molybdate melt has a useful characteristic, which is an ability to dissolve uranium oxides for a short time.[1] In the previous study[2], it was confirmed by the absorption spectrophotometry of the dissolved uranium species in the molten Li_2MoO_4–Na_2MoO_4 eutectic at 550 °C that the uranium species in the melt existed as the uranyl penta-valent ion UO_2^+, when UO_2 was dissolved into the melt. And after purging oxygen gas into the melt, we could observe that UO_2^+ was oxidized to the uranyl hexa-valent ion, UO_2^{2+}. In this study, the redox reactions of the dissolved uranium species in the melt were measured by cyclic voltammetry.

EXPERIMENTS: All the measurements were carried out in a glove box filled with argon gas whose humidity and oxygen were kept less than 1 ppm. The measurement temperature of the melt was kept at 550±1 °C by an automatically controlled electric furnace. Anhydrous Li_2MoO_4 and Na_2MoO_4 of purity 99 % up were purchased from Kojundo Chemical Lab. Co., Ltd. and processed by the vacuum drying at 150 °C before use. The Li_2MoO_4–Na_2MoO_4 eutectic was prepared by melting the mixed anhydrous reagents of Li_2MoO_4 and Na_2MoO_4 at 750 °C. The UO_2 powder was dissolved into molten Li_2MoO_4–Na_2MoO_4 eutectic by adding MoO_3. Then this source material containing uranium species was added into the measurement melt.

   In the cyclic voltammetry, about 10 g of the prepared Li_2MoO_4–Na_2MoO_4 eutectic and the uranium source material were put into the measurement cell made of quartz tube and heated to 550 °C. After melting was completed, three electrodes were all inserted into the measurement cell: a working, a counter and a reference electrode. Two platinum wires were used as the working and counter electrode. The reference electrode utilized was composed of a Pyrex tube with about 1 g of 12.17 mol% MoO_3 in Li_2MoO_4–Na_2MoO_4 eutectic and a platinum wire.

RESULTS: Figure 1 shows the cyclic voltammograms of uranium species in molten Li_2MoO_4–Na_2MoO_4 eutectic for various measuring potential ranges. The UO_2 concentration in the melt was 1.02 mol%. The reductive reactions of uranium species in the melt were observed in a potential range that was more negative than 0.1 V as shown Ic, IIc and IIIc in Fig. 1, and the oxidizing reac-

tions were observed in Ia, IIa, IIIa, and IIIa' in Fig. 1.

   The reductive reaction of Ic and oxidizing reaction of Ia are presumed to be the redox reaction of the UO_2^{2+}/UO_2^+ couple, because the existence of the uranyl ions, UO_2^+ and UO_2^{2+}, in the melt was confirmed by the absorption spectrophotometry in previous study[2]. To confirm that this redox reaction is a soluble–soluble reaction, cyclic voltammograms in potential range of −0.25 to 0.4 V were measured for various potential sweep rates. The reductive current of reaction Ic included other reactions, but the current density of this redox couple increased with an increase of the potential sweep rate. As for oxidizing reaction of Ia, the relation between the square root of potential sweep rate and the oxidizing current density showed a good linearity.

   The deposition current peak of uranium species in the melt was observed in a potential range that was more negative than −0.45 V shown as IIIc, and the dissolution current peak of deposited uranium compounds on the working electrode was observed below −0.3 to −0.4 V shown as IIIa and IIIa'. And reductive reaction of IIc below −0.4 to −0.3 V and oxidizing reaction of IIa over −0.15 to 0 V accounted for deposition of other uranium species and dissolution of uranium compounds.
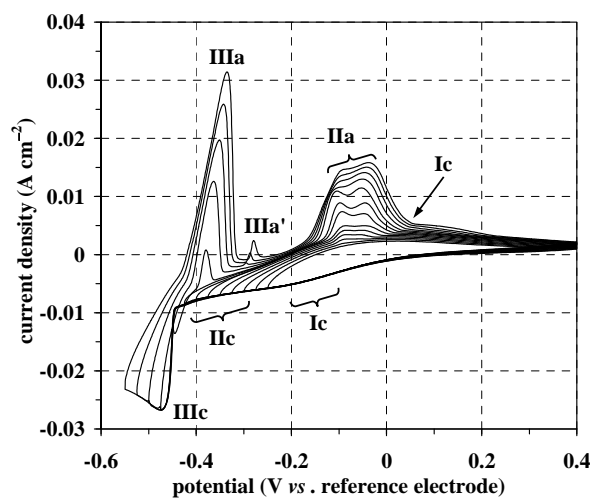

Fig. 1.   Cyclic voltammograms of dissolved uranium species in molten Li_2MoO_4–Na_2MoO_4 eutectic at 550 °C for various measuring potential ranges. UO_2 concentration in the melt was 1.02 mol%. Potential sweep rate: 10 mV s^{-1}.

REFERENCES:
[1] K. Mizuguchi, Y. Yasuike, M. Fukushima, M. Myochin, *Trans. At. Energy Soc. Japan*, Vol.6, No.4, pp.484-490 (2007), [in Japanese].
[2] T. Nagai, M. Fukushima, A. Uehara, T. Fujii, M. Myochin, H. Yamana, *2008FY KURRI progress report*, PR4-9 (2009).

PR4-8   Electrolytic Reduction of UO_2 in LiCl Salt Bath at 923 and 973 K

Y. Sakamura[1], T. Fujii[2], A. Uehara[2] and H. Yamana[2]

[1]*Central Research Institute of Electric Power Industry*
[2]*Research Reactor Institute, Kyoto University*

INTRODUCTION: In the electrolytic reduction process of actinide oxides, which has been developed for pyrochemical reprocessing, the anode and cathode reactions are described as follows:

$$\text{Cathode:} \quad MO_2 + 4\,e^- \rightarrow M + 2\,O^{2-} \qquad (1)$$
$$\text{Anode:} \quad 2\,O^{2-} \rightarrow O_2 + 4\,e^- \qquad (2)$$
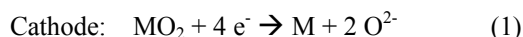
where M denotes actinides such as U and Pu. At the cathode, actinide oxide is reduced to metal. The ionized O^{2-} is transported through the salt and then discharges at the anode to form O_2 gas. It has been demonstrated that UO_2 and UO_2-PuO_2 (MOX) can be reduced to their metals in molten LiCl salt bath at 923K [1-3]. In this study, temperature effect on the reduction rate of UO_2 was investigated.

EXPERIMENTS: A schematic diagram of the experimental cell located in a high-purity Ar atmosphere glove box is shown in Fig. 1. A LiCl-0.7mol%Li_2O melt was contained in a MgO crucible. The UO_2 electrode consisted of a fragment of UO_2 disk (~0.2 g) wound with Ni wires. A Pt sheet was employed as the counter electrode. The reference electrode consisted of a Ta wire immersed in a liquid Li-Bi alloy (30 mol%Li) of which potential was often checked against a Li metal electrodeposited on a Ni wire. The potential used in this paper is relative to the Li/Li^+ couple, unless otherwise stated.

Three UO_2 reduction tests were carried out by constant potential electrolysis at 0.02 V (vs. Li/Li^+) until UO_2 was completely reduced to U metal. Temperature was 923 K for Run 1 and 973 K for Run 2 and Run 3.

RESULTS: Figure 2 shows cyclic voltammograms (CVs) for UO_2 electrodes at 923 and 973 K. A cathodic current rising steeply at 0.00 V and a sharp anodic wave at about 0.02 V are due to the reduction of Li^+ and the anodic dissolution of the deposited Li metal, respectively.

$$Li^+ + e^- \leftrightarrow Li \qquad (3)$$

A cathodic current rises at about 0.15 V is due to the reduction of UO_2 to U metal described by Eq.(1), and the anodic wave at 0.20 V might be due to the oxidation of the U metal to UO_2. It is obvious that the current corresponding to the UO_2 reduction was larger at 973 K than at 923 K.

Figure 3 shows the change in current during electrolysis. The current-time curve for Run 1 at 923 K reached a plateau at about 7 mA after 9500 s had passed, indicating that the UO_2 reduction was completed. As for the

electrolysis at 973 K, the current was larger and the UO_2 reduction seemed to be completed in 5300 s. After the electrolysis, the products were cut and cross sections were observed with an optical microscope. It was verified that there was no UO_2 remained in the three products.

It was concluded that the reduction rate of UO_2 was almost twice as high at 973 K as at 923 K. However, at higher temperature, more LiCl electrolyte evaporates during the operation, which has to be taken into account.

REFERENCES:
[1] Y. Sakamura *et al.*, J. Electrochem. Soc. **153** (2006) D31.
[2] M. Iizuka *et al.*, J. Nucl. Mater. **359** (2006) 102.
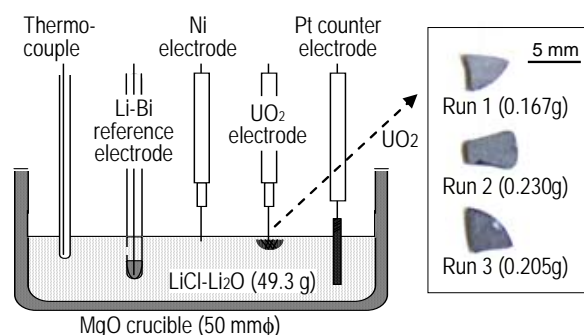[3] Y. Sakamura *et al.*, Nucl. Technol. **162** (2008) 169.

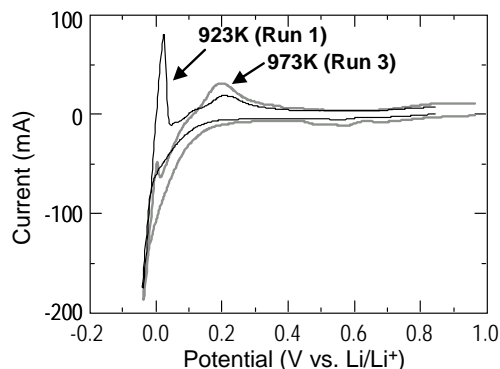Fig. 1   Schematic diagram of the experimental cell.

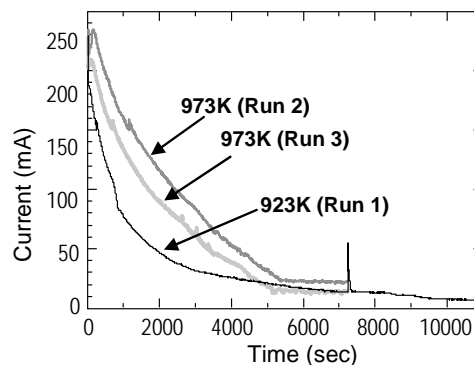Fig. 2   Cyclic voltammograms of UO_2 electrodes in LiCl-Li_2O at 923 and 973 K. Scan rate: 0.05 mV/s.

Fig. 3   Current-time curves during potentiostatic electrolysis (0.02 V vs. Li/Li+) of UO_2 in LiCl-Li_2O at 923 and 973 K.

PR4-9   Solvent Extraction of Trivalent Actinum, Americium, Curium, and Californium with Di(2-ethylhexyl)Phosphoric Acid

R. Takayama[1], Y. Kikutani[1], K. Ooe[1], H. Fujisawa[1],
Y. Komori[1], A. Kuriyama[1], H. Kikunaga[1], T. Yoshimura[1],
N. Takahashi[1], K. Takamiya[3], T. Mitsugashira[2] and
A. Shinohara[1]

[1]*Graduate School of Science, Osaka University*
[2]*Institute of Materials Research, Tohoku University*
[3]*Research Reactor Institute, Kyoto University*

INTRODUCTION: Among actinides, Pa, U, Pu, and Np show various oxidation states because 5f electrons are less localized in the inner sphere of the atomic orbital compared with 4f electrons. On the other hand, lanthanides and heavy actinides from Am to Lr except No have stable oxidation state of +3. Therefore, their chemical properties of trivalent actinides and lanthanides are very similar one another and the chemical properties sometimes depend largely on the ionic radii. It is found that the chemical properties of trivalent actinides are slightly different from those of trivalent lanthanides by the effect of f electrons. For example, the soft donor such as sulfide favors to bind to trivalent actinide over lanthanide. These chemical behaviors are not able to be explained only by the ionic radii. It is interesting to study chemical properties of the trivalent actinides to clarify the effects from the 5f electrons. In the present work, the extraction behavior of Ac(III), Am(III), Cm(III), and Cf(III), into di(2-ethylhexyl)phosphoric acid (HDEHP) was studied together with lanthanides under the same conditions to clarify the difference of the tetrad effect between the lanthanide and actinide series.

EXPERIMENTS: The isotope ^{228}Ac was separated from ^{228}Ra as described below. A 50 kBq of ^{228}Ra was supplied from Kyoto University Research Reactor Institute. The ^{228}Ra was dissolved in 0.1 M HNO$_3$. The solution was passed through a column in which Radium Rad Disks (3M) was packed, which absorbed ^{228}Ra. The column was washed with 0.1 M HNO$_3$ to flush out ^{228}Ac completely. For the extraction, an aqueous solution of HNO$_3$ containing tracer amounts of Ac(III), Am(III), Cm(III), Cf(III), Ce(III), and Eu(III) were used. The ^{139}Ce and ^{152}Eu tracers were used to confirm the extraction behavior of Ln(III). The aqueous solution was added to 0.2-0.8 M of HDEHP in benzene. The mixture was shaken and then each phase was separated. The distribution ratios were obtained by measuring the radioactivities of ^{228}Ac, ^{241}Am, ^{243}Cm, and ^{251}Cf in the both phases by γ-ray spectrometry with high-purity Ge detectors.

RESULTS: Figure 1 shows the plots of log$D$ against log[HDEHP]$_2$. In all of the trivalent lanthanides and actinides in this study, the slope values are almost +3. The results indicate that each of the trivalent lanthanides and
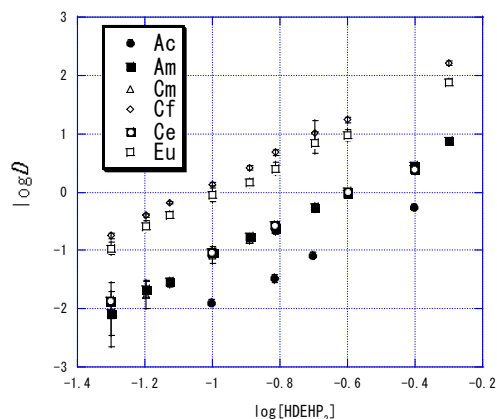

Fig. 1. The distribution ratio (log$D$) versus log[HDEHP$_2$] in 0.1 M HNO$_3$-benzene.
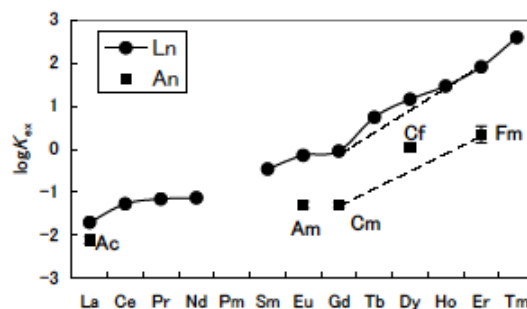

Fig. 2. The logK_{ex} values of trivalent lanthanide (except for Pm) and Ac, Am, Cm, Cf, and Fm.

actinides formed the complex with [HDEHP]$_2$ in a 1:3 molar ratio and the complex was extracted to the organic phase. Fig. 2 shows the K_{ex} value of lanthanides and actinides in HNO$_3$/HDEHP-benzene solution. The plot clearly shows that the K_{ex} values of actinides are significantly smaller than those of the isoelectronic lanthanides. In actinide series, K_{ex} values are increased in the order Ac(III) < Am(III) ≈ Cm(III) < Cf(III) ≈ Fm(III). An interesting trend was found when the extraction behavior of lanthanides and actinides having similar ionic radii was compared; the K_{ex} value of Cf (0.95 Å of C.N. =6) is larger than that of Eu(0.947 Å), whereas the K_{ex} values of Am(0.975 Å) and Cm(0.97 Å) are smaller than those of Nd and Sm, respectively. The difference of the K_{ex} value between Fm(0.911 Å) and Ho (0.901 Å) shows the similar trend to the relation between Am/Cm and Nd/Sm. This finding could be responsible for a stronger tetrad effect to trivalent actinides compared with lanthanides in the HDEHP system.